In-situ structural investigations of ferroelasticity in soft and hard rhombohedral and tetragonal PZT

Maxim. I. Morozov[1,a)] , Mari-Ann Einarsrud[1], Julian R. Tolchard[1], Philipp T. Geiger[2], Kyle G. Webber[2], Dragan Damjanovic[3], and Tor Grande[1]

[1]*Department of Materials Science and Engineering, Norwegian University of Science and Technology, NO-7491 Trondheim, Norway*

[2] *Department of Materials Science, Friedrich-Alexander-Universität Erlangen-Nürnberg, 91058 Erlangen, Germany*

[3] *Ceramics Laboratory, Swiss Federal Institute of Technology in Lausanne-EPFL, 1015 Lausanne, Switzerland*

Despite the technological importance of hard and soft PZT, $Pb(Zr,Ti)O_3$, ceramics, the mechanisms of ferroelectric hardening and softening remain widely discussed in literature. The hardening and softening phenomena have traditionally been investigated in relation with dielectric manifestations such as aging of the dielectric susceptibility and constriction of the polarization-electric field hysteresis loop. Here we present a systematic investigation of the ferroelectric and ferroelastic properties of soft and hard PZT in both the tetragonal and rhombohedral phases. A particular focus has been devoted to ferroelastic domain switching by characterizing the macroscopic mechanical constitutive behavior and *in-situ* synchrotron X-ray

a) Corresponding author, e-mail: maximm@alumni.ntnu.no

diffraction during compression. It is demonstrated that variation of the ordering state of point defects in PZT ceramics affects the switching behavior of both ferroelectric and ferroelastic domains under mechanical or electrical fields. Softening of the mechanical and electrical properties of originally hard PZT ceramics was conferred by quenching the materials from above the Curie temperature. The present findings are discussed with respect to the current understanding of hardening-softening transitions in ferroelectric materials.

I. INTRODUCTION

Introduction of donor or acceptor dopants in lead zirconate titanate (PZT) is one of the most successful methods to tailor the piezoelectric and ferroelectric performance of these electroceramics.[1] Aliovalent dopants can control both the intrinsic and extrinsic properties, such as bulk electric conductivity and mobility of domain walls. Acceptor doping is known to induce ferroelectric "hardening", i.e. weakening of dielectric and electromechanical properties, accompanied with lowering their nonlinearity and hysteresis. In contrast, donor dopants typically result in "softening" effects with the opposite tendencies. Many theoretical and experimental studies have been dedicated to these phenomena and several models have been proposed to describe the dielectric nonlinearity and hysteresis using phenomenological, micromechanical, and statistical simulations.

The phenomenological models of "hardening" usually consider interaction between the spontaneous polarization (P_S) and charged point defects, whose collective ordering or localization

results in pinning of domain walls, hence reducing their mobility. Several models with different localizations of charged point defects (in some models – space charge) have been proposed and discussed extensively.[2-16] Ordering of charged point defects with respect to polarization is a result of their interaction with Ps at elevated temperatures below the Curie temperature, T_C. Migration and rearrangement of mobile point defects may occur quickly[17,18] at the last stage of thermal processing, when sintered ceramics first reach the polar state on cooling below T_C. At room temperature the ordered arrangement of the point defects is considered to be "frozen", thus their collective interaction with P_S tends to hold the domain configuration stable, manifesting itself as a "restoring force" for the motion of weak domain walls. In case of "hard" acceptor-doped ceramics, positively charged oxygen vacancies $V_O^{\bullet\bullet}$ appear to balance partially or completely[18-20] the negatively charged acceptors. Due to certain mobility below the Curie temperature (e.g. in PZT, T_C > 300 °C), $V_O^{\bullet\bullet}$ - acceptor pairs may adopt preferential sites in the unit cells with respect to the spontaneous polarization of the ferroelectric domains. Thus the level of charged point defect ordering can be a measure of ferroelectric hardening.

Unlike "hardening", the "softening" mechanism is still poorly understood. It is believed that undoped ceramics are "hard" to a certain extent, i.e. due to the presence of $V_O^{\bullet\bullet}$ mainly owing to loss of PbO. The $V_{Pb}'' - V_O^{\bullet\bullet}$ pair then has a similar role in hardening as the acceptor dopant-oxygen vacancy cluster. The introduction of donor dopants (i.e. Nb^{5+}) reduces this natural ferroelectric "hardness" by reducing the number of oxygen vacancies and thus manifests itself as softening. Whether any additional softening effects, beyond the decrease in concentration of oxygen vacancies, are present is currently not understood. The softening donor-type dopants in PZT are typically cation substitutes (e.g. $Nb_{(Zr,Ti)}^{\bullet}$) balanced by cation vacancies (e.g. V_{Pb}''). These two point defects are considered to be immobile compared to oxygen vacancies at temperatures below T_C, thus they are not able to become ordered with the onset of the spontaneous polarization

below T_C. Moreover, recent first principle calculations[21] show that $V''_{Pb} - Nb^{\bullet}_{Ti}$ pairs are weakly bound, that is, there is no tendency to form a cluster that could align itself with polarization. The level of disorder in the distribution of charged point defects can therefore be a measure of ferroelectric softening.

To summarize, the collective ordering of charged point defects in a hard ferroelectric system is understood as the origin of the domain wall pinning, opposed to soft ferroelectric systems with a random (disordered) distribution of charged point defects.

The phenomenological link between the degree of order-disorder in the arrangement of charged defects, which constitute the pinning environment for the domain walls and thus the energy landscape for their movement, and the empirically observed hardening-softening of the corresponding ferroelectric properties gave rise to a model of hardening-softening transition.[17,22] The model links the level of hardening-softening of a ferroelectric system with the steepness, roughness, and randomness of the potential energy profile for domain wall movement. In the limiting cases corresponding to extremely hard or soft states of a ferroelectric system, the potential energy landscapes can be described by various modifications of a so-called "V-potential" (single potential well for a domain wall in a hard material)[11,23] or by random potential energy profile (Rayleigh model) for a soft material.[24-27] Therefore, many intermediate states of a ferroelectric system constitute a variety of gradual transformations of potential energy profile with variable steepness, randomness, and roughness.[17,22]

An important implementation of the aforementioned qualitative model is that the extrinsic properties of multidomain ferroics may be smoothly and gradually controlled by the rearrangement of charged point defects. In practice, this can be realized by either proper dopant choice (e.g., type, concentration, and mobility of the charge carriers at elevated temperature), softening originally hard ceramics by thermal quenching, cycling at switching electric fields, or

vice-versa – hardening acceptor doped ceramics by slow thermal relaxation without applying fields. [2,17,29] Note that such manipulations have no effect on soft materials where defects have no tendency to form defect clusters orienting with respect to polarization or strain. These and other experimental verifications of the model have been performed in various ferroelectrics, including hardening of PZT,[2,12,14,17,28-30] $BaTiO_3$,[5,12-15,16] $BiFeO_3$,[31-33] $(K,Na)NbO_3$,[34] Aurivillius layered perovskites,[35] and others.[2,36,37] The key property considered in such studies has typically been the P-E hysteresis loop, the polarization response to cyclically applied electric field, as systematically summarized in a recent review by Jin.[37] Although the electromechanical and mechanical properties have also been reported for hard and soft ferroelectrics,[38-47] they are rarely and less systematically addressed in the literature with respect to hardening-softening transitions. In particular, the mechanisms of hardening and softening such as pinning of ferroelastic domains by electrostatic, electromechanical, or purely elastic interactions with point defects still need to be addressed in detail.

In this study we report on the ferroelectric and ferroelastic properties of soft and hard tetragonal and rhombohedral PZT ceramics. The effect of thermal quenching of hard PZT from above T_C on the mechanical properties is also included. Ferroelastic domain switching under a uniaxial compressive load is investigated by *in-situ* synchrotron X-ray diffraction. Here we systematically address both the ferroelastic and ferroelectric properties in soft and hard PZT with respect to defect ordering in both tetragonal and rhombohedral phases. The study is therefore complementary to the model of hardening-softening transitions[17,22] in ferroelectric ceramics with an emphasis on the mechanical (stress-strain) relationships.

II. EXPERIMENTAL

Dense ceramics of rhombohedral (58/42) $Pb(Zr_{0.58}Ti_{0.42})O_3$ and tetragonal (42/58) $Pb(Zr_{0.42}Ti_{0.58})O_3$ were prepared by conventional solid state process described elsewhere.[17] Hard and soft PZT were prepared by substitution of 1 at.% Fe and 1 at.% Nb at the B-site, respectively. The base rhombohedral PZT (58/42) composition was chosen for a series of studies dedicated to the hardening-softening phenomenon,[17,28-30] following the original study by Carl and Härdtl.[2] The base tetragonal PZT (42/58) composition is sufficiently distant from the morphotropic phase boundary composition region to avoid complications in interpretation related to mixed phases and monoclinic structures. Both the rhombohedral and tetragonal compositions have already been preliminary investigated previously[17] mainly focusing on the dielectric phenomena.

The sintered cylindrical pellets of ~0.8 mm height and ~4 mm diameter were electroded with sputtered gold and subjected to electrical characterization. Another set of samples was prepared for mechanical testing with ~5-6 mm height and ~6 mm diameter by core drilling samples from a sintered block. Finally, samples of ~4 mm height and ~4 mm diameter were prepared for mechanical testing combined with a synchrotron diffraction examination. In order to remove residual stresses after mechanical treatments, all samples were annealed at 500-600 °C followed by a slow relaxation cooling within the furnace and aging at room temperature for 1 day or longer. Prior to measurements, some of the hard PZT samples were thermally quenched by heating to 450 °C followed by quenching by dropping the samples into water at room temperature. These samples are referred to as “hard-quenched” or “softened”.

Poling and examination under driving electric field (triangular waveform, 0.25 Hz) were performed using an aixPES – Piezoelectric Evaluation System (aixACCT Systems GmbH, Aachen, Germany). The direct piezoelectric coefficient d33 was measured with a d33-meter (90-2030, APC Products Inc, Mackeyville, PA, USA). All characterizations, except d33, were performed with unpoled samples. For d33 characterizations, the rhombohedral samples were poled as follows: hard – at 25 kV/cm, 100 °C, for 10 min, then cooling under field; soft and hard

quenched – by a few short unipolar pulses at 50 kV/cm, room temperature. The poling procedure was adjusted with respect to the optimal conditions for obtaining high remnant polarization, though avoiding substantial dc leakage.[17]

Mechanical testing under compressive stress was performed using an experimental setup described in detail elsewhere.[44] A compressive stress up to 500 MPa with a rate of 5 MPa/s was applied to the preloaded (~5 MPa) specimen centered by an alumina alignment fixture. After reaching the maximum compressive stress, the specimen was unloaded with the same loading rate back to the preload stress. The stress-induced uniaxial displacement of the specimen was measured by a linear variable differential transformer (LVDT).

The outer flat surface of the cylindrical samples was investigated before and immediately after the mechanical testing by *ex-situ* X-ray diffraction (XRD; Siemens D5005 diffractometer with CuKα-radiation and secondary monochromator, Karlsruhe, Germany).

In-situ X-ray diffraction during compression-decompression cycles was performed at the ID15B beamline of the European Synchrotron Radiation Facility (ESRF). An X-ray beam with a wavelength of 0.1424 Å was confined in the horizontal direction. The cylindrical specimens were mounted in a 4.4 kN Instron hydraulic stress rig. The cylindrical samples were mounted with the cylindrical axis vertical in the stress rig, perpendicular to the incident X-ray beam, as schematically illustrated in Fig. 1. The position of the beam was adjusted to the centre of the cylinders by measuring the absorption across the specimen. The mechanical load during compression and decompression was changed manually stepwise by small increments ~0.3 MPa/s each step, followed by recording the diffraction patterns. The diffraction rings were recorded with a large-area detector system. The detector system was placed at a distance of 1273 mm away from the specimen and coupled to a CCD camera with an effective pixel size of 154 μm. The diffraction data were processed as described elsewhere,[48] using FIT2D software.[49,50]

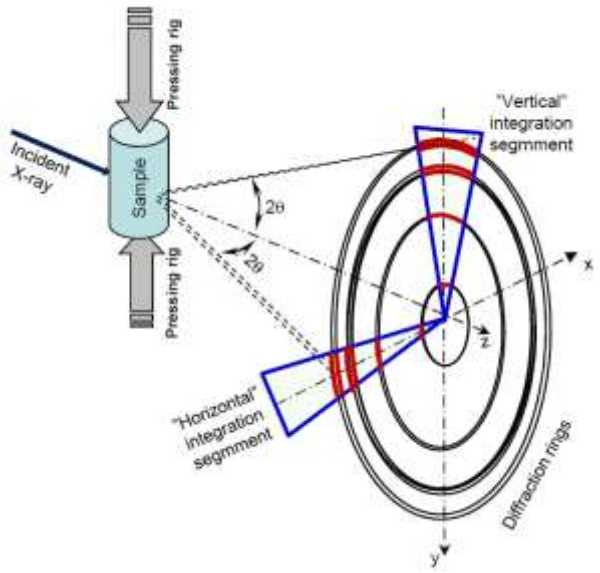

FIG. 1 Experimental setup for *in-situ* X-ray diffraction during compression-decompression cycles.

III. RESULTS AND DISCUSSION

The large signal dielectric (P-E), electromechanical (S-E), and mechanical (S-□) hysteresis loops are shown in Fig. 2 for the hard, soft, and softened (hard-quenched) rhombohedral (58/42) and tetragonal (42/58) PZT ceramics. As a general trend, the amplitude of hysteretic response (polarization and strain) is higher for the soft PZT ceramics and lower for the hard compositions. After quenching, the originally hard ceramics became softer and demonstrated a notable enhancement of the response amplitudes, though still not as high as the soft (Nb-doped) ceramics. This is consistent with the model of hardening-softening transitions, as thermal quenching hinders ordering of point defects below T_C and thus prevents pinning of domain walls.[29] Thus it is feasible, that with finite rate of cooling the distribution of the originally ordered point defects will, after quenching, approach, but may not fully achieve, the level of disorder pertinent to the soft systems. The random distribution of defects in the soft systems is

established at higher temperatures far above T_C, in the absence of spontaneous polarization; it is thus remarkable that the polarizations of donor-doped and quenched acceptor doped materials are so similar.

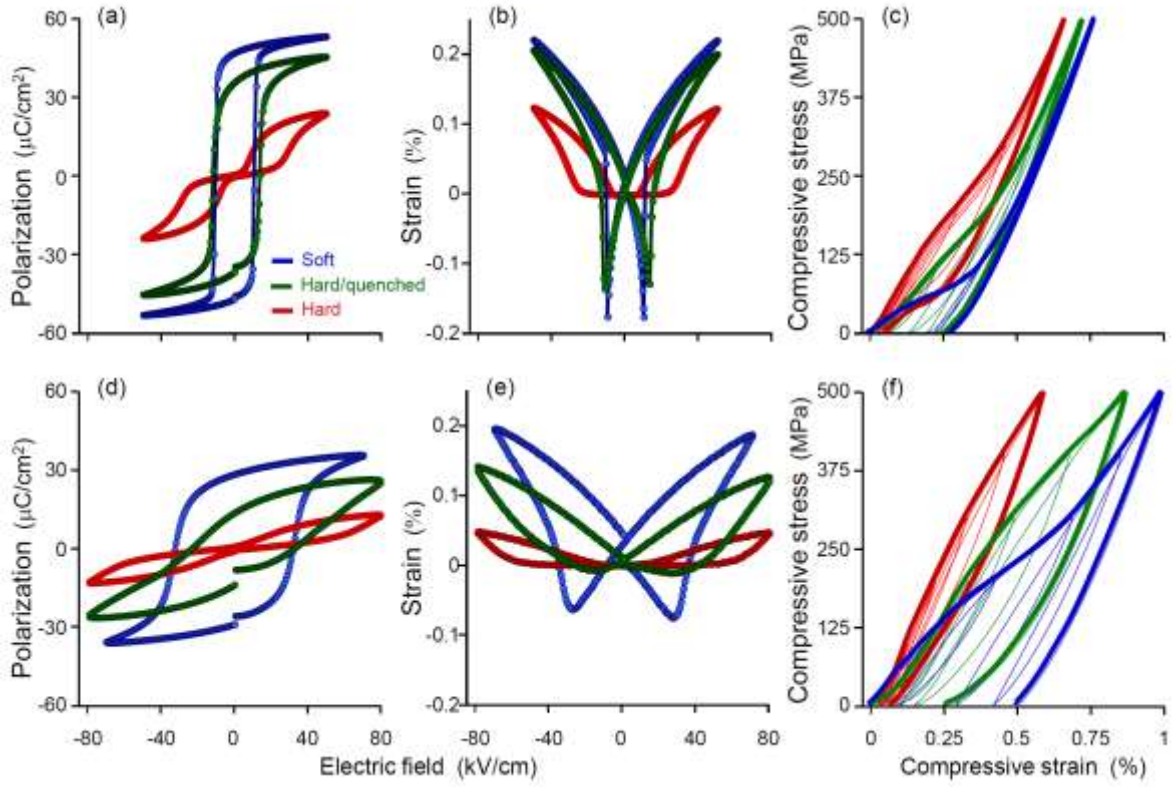

FIG. 2 Hysteresis loops in rhombohedral 58/42 (a-c) and tetragonal 42/58 (d-f) PZT ceramics. Thin lines on panels (c) and (f) correspond to the cycles of the stepwise increasing stress amplitude; thick lines emphasize the last measured cycle with the highest stress amplitude.

A similar tendency was observed in reversibility of the induced electrical and mechanical responses. Both P-E (Fig. 2 (a,d)) and S-σ (Fig. 2 (c,f)) hysteresis loops are closed (pinched) in the case of hard ceramics, showing nearly zero remanent polarization and strain. Thermal quenching results in irreversibility of the responses, manifested by open hysteresis loops and induced remanence, similar to those observed in soft materials. The highest remanence is observed in soft ceramics. The same tendency was observed at the primary unipolar S-E cycles (not shown).

Another common feature observed in all hysteresis loops in Fig. 2 is the higher coercive fields in tetragonal compositions compared to rhombohedral. As the tetragonal phase possesses higher lattice distortion than the rhombohedral phase (larger tetragonal d_{100}/d_{010} than rhombohedral d_{021}/d_{003} lattice spacing ratios), and taking into account different available orientations for the P_S in the lattice (six in tetragonal and eight in rhombohedral material), it is also feasible that the tetragonal ceramics is naturally harder with respect to domain reorientation relative to rhombohedral compositions. Under mechanical compression, the tetragonal ceramics showed higher remanent strain compared to the rhombohedral ceramics (Fig. 2 (c,f)). In contrast, under electric field cycling, the rhombohedral ceramics demonstrated higher maximum strain compared to tetragonal ceramics (Fig. 2 (b,e)). This feature suggests higher intrinsic contribution to the electromechanical response for the rhombohedral samples, in terms of the corresponding mechanisms pertinent to the tetragonal "extenders" (polarization extension/contraction) and the rhombohedral "rotators" (polarization rotation).[52]

TABLE I. Small-signal parameters of dielectric and direct piezoelectric coefficients measured in hard and soft $PbZr_{0.58}Ti_{0.42}O_3$ ceramics: initial values and Rayleigh coefficients. From ref.[17]

Sample:	"Hard"	"Hard-quenched"	"Soft"
ε_r^{init} (-)	520	650	550
α_ε (mm/V)	0.2	0.7	3.5
d_{33} (pm/V) $^{(*)}$	120	150	185
d_{33}^{init} (pm/V)	110	-	170
α_d ($pC \cdot mm^2/N^2$)	11	-	58

$^{(*)}$ this study: measured by a Berlincourt method at ~10N load.

The switching hysteresis processes illustrated in Fig. 2 are qualitatively consistent with the behavior of non-linear dielectric and piezoelectric properties measured at sub-switching conditions and listed in Table I. The amplitude dependence of a dielectric or piezoelectric response at a given frequency can be interpolated and analyzed using Rayleigh formalism:[24,52,53]

$$\varepsilon_r = \varepsilon_r^{init} + \alpha_\varepsilon E_0$$

$$d_{33} = d_{33}^{init} + \alpha_d \sigma_0$$

where E_0, σ_0 are the amplitudes of applied ac electric field or mechanical stress; ε_r and d_{33} are the relative dielectric permittivity and the direct piezoelectric coefficient; ε_r^{init}, d_{33}^{init} and α_ε, α_d are their corresponding initial values at zero field amplitude and the Rayleigh coefficients. The Rayleigh coefficients are a measure of the extent of irreversible domain wall displacement under an applied ac force,[22] while the initial values account for all reversible contributions, including the intrinsic lattice response. Thus the Rayleigh coefficients α_ε and α_d listed in Table I demonstrate the same tendency of increasing contribution of irreversible domain wall motions with softening of a ferroelectric system correlated with the expected disordering in the distribution of charged point defects. Note, that correct assessment of the piezoelectric nonlinearity for thermally quenched samples could not be performed using the Rayleigh model, since the frozen disorder of point defects induced by quenching would be affected by the poling procedure as well as the poling temperature.

In order to address the microscopic domain switching processes in the ceramics under investigation, we next analyze the *in-situ* X-ray diffraction patterns recorded during the

mechanical compression-decompression cycling. Representative measurements for soft rhombohedral PZT are shown in Fig. 3, where the progression of the (003) and (021) reflections are shown at different stages during a compression-decompression cycle. Under uniaxial compression, the intensity ratio between these two reflections in the vertical (Fig. 3 (a)) and horizontal (Fig. 3 (b)) integration segments changes, following the ferroelastic switching of domains with the spontaneous strain tending to align as close to the horizontal plane as possible. For the soft rhombohedral ceramics, the intensity ratios remained almost unchanged after release of the compressional force, thus demonstrating the low level of back-switching of the ferroelastic domains occurred in soft material during unloading.

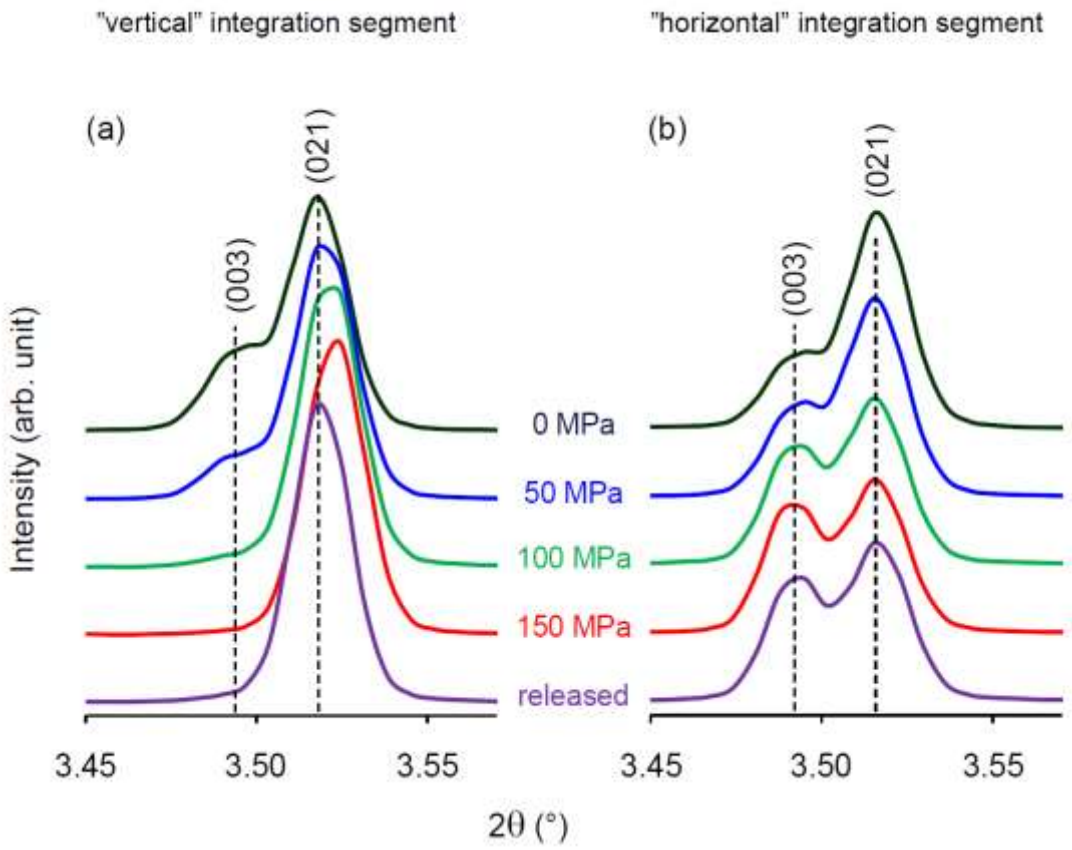

FIG. 3 X-ray diffraction patterns of the soft PZT (58/42) ceramics during loading-unloading cycles integrated in the (a) vertical and (b) horizontal segments.

The evolution of the d-spacing and relative intensities of reflections demonstrating ferroelastic domain switching is shown in Figure 4. For the rhombohedral materials (space group *R3m*) the intensity of (003) and (021) reflections relative to the intensity of the reflection (202) is displayed together with the relative shift of d_{202} with increasing load. For the tetragonal materials (space group *P4mm*), the intensity ratio of the reflections (200) and (002) relative to (111) and the relative d-spacing shift of d_{111} are displayed as a function of the mechanical field. The intensities are normalized to the intensity of a Bragg reflection, the intensity of which was not influenced by domain switching. The panels (a-c) correspond to the rhombohedral ceramics, and (e-f) to the tetragonal materials. Due to mechanical failure at high compression loads, some of the curves illustrate only the compression part of the cycles, except for the rhombohedral-soft and the tetragonal-quenched samples, measured during decompression as well.

For soft and hard rhombohedral PZT the intensity of (003) peak in the vertical integration segment of the diffraction ring is reduced, while the intensity of (021) peak is enhanced with increasing load (Fig. 4(a)). This tendency reflects the ferroelastic domain switching during increasing mechanical load. The initial intensity ratio of these two reflections is roughly ~1:3, indicating the splitting of the cubic (111) reflection due to the rhombohedral distortion and the 8 possible orientation of the polarization. Upon loading the domains oriented in favor of the mechanical field are stabilized, while domains with an unfavorable crystallographic orientation are switched to an orientation in favor of the field, resulting in a suppression of the intensity of (003) and enhancement of the intensity of (021), as demonstrated in Fig 4(a). Perpendicular to the applied mechanical field (Fig. 4 (b)), the opposite trend is observed with reduction of the intensity of (021) and an increase in the intensity of (003). The change in the intensity ratio is shifted to higher load for hard PZT, confirming a significant higher coercive field of hard PZT relative to soft PZT. Compression is also shown to be accompanied with a significant negative or positive strain, dependent on the orientation relative to the mechanical field (Fig 3(c)).

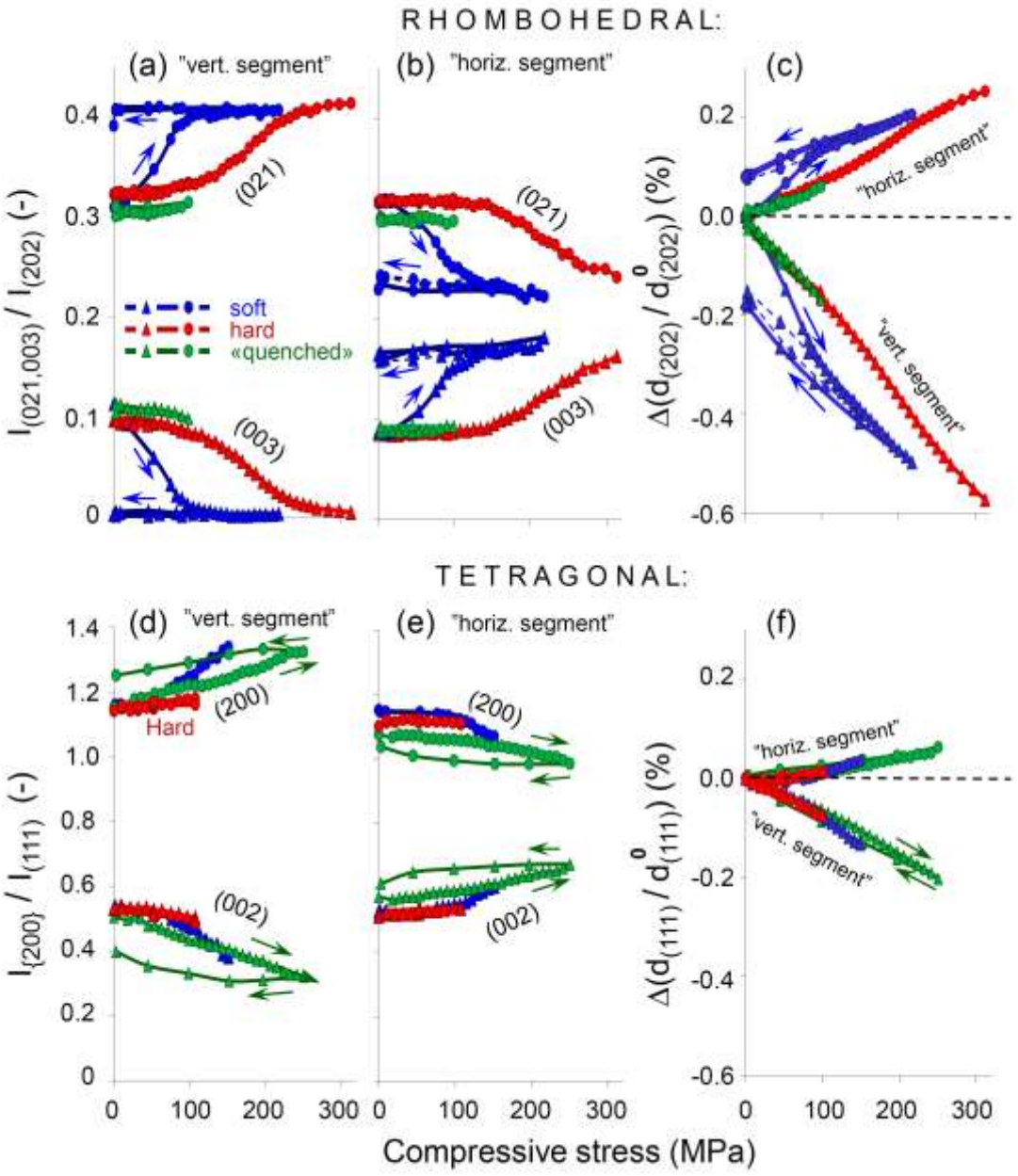

FIG. 4 X-ray diffraction analysis of hard, soft, and quenched-soften PZT ceramics under mechanical compression-decompression. Rhombohedral PZT ceramics: Evolution of the relative intensity of the (003) and (021) reflection normalized in the (a) vertical and (b) horizontal integration segment; (c) the relative change in the d_{202} lattice spacing for rhombohedral PZT. Tetragonal PZT ceramics: Evolution of the relative intensity of (200) and (002) reflections normalized by the intensity of (111) in the (d) vertical and (e) horizontal integration segment; (f) the relative change in the d_{111} lattice spacing for tetragonal PZT.

For tetragonal PZT the intensity of (002) is enhanced while the intensity of (200) is suppressed in the vertical segment, as shown in Fig. 4(d), confirming the ferroelastic domain

switching under compression and a higher coercive field for hard PZT. In the perpendicular direction (Fig. 4(e)), the opposite trend is observed, corresponding to observations in the rhombohedral composition. In addition, a lattice strain is observed associated with the compression, Fig. 4 (f).

Thus, the evolution of the reflection intensities shown in Fig. 4 (a,b) and Fig 4 (d,e) for the rhombohedral and tetragonal compositions confirms the microscopic ferroelastic domain switching of the macroscopic stress-strain behavior. The stress-derivation of either the macroscopic strain curves shown in Fig. 2 (c) or the intensity ratio shown in Fig 4 (a,b) yield similar values of the coercive stresses: ~ 50 MPa for the soft and ~250 MPa for the hard rhombohedral PZT ceramics. Since these values have been obtained for the PZT (58/42) ceramics modified with the fixed (1%) concentration of Fe and Nb dopants, the coercive stress and the remnant strain therefore can be controlled within the indicated range by hardening-softening manipulations.

The evolution of the reflection intensities of the soft rhombohedral PZT ceramics showed an essentially irreversible alternation during the complete compression-decompression cycle in the both vertical and horizontal integration segments (Fig. 3 (a,b) and Fig. 4 (a,b). These results demonstrate that the material did not show significant back-switching of the ferroelastic domains. As will be shown next, this is not the case for the hard PZT ceramics.

In order to link the macroscopic stress-strain behavior and the ferroelastic domain switching observed by *in-situ* X-ray diffraction, we now compare the results of two different experiments shown in Fig. 5 for the hard, hard-quenched, and soft rhombohedral PZT ceramics. The stress-strain characterization (Fig. 5 (a)) is thus combined with analysis of X-ray diffraction in the transmission mode (Fig. 5(b)). As discussed previously, the ceramics with different state of point defect ordering exhibited different levels of remanent strain induced by the primary cycle of uniaxial compression. For a maximum compressive stress of 100 MPa, the soft ceramic showed

the largest ferroelastic response, noted by the largest remanent strain and lowest coercive stress. In contrast, the hard ceramic displayed neither significant ferroelastic hysteresis or strain remanence, while thermal quenching resulted in the softening (Fig. 5 (a)). The reorientation of domains changes the intensities of the (003) and (021) reflections. In case of the "vertical" integration segment (Fig. 5 (b)) the intensity of the reflection at lower 2θ angle (higher d-value) decreases under compression, while the intensity of the neighbor reflection at higher 2θ (lower d-value) increases. Quantitatively, the intensity of the (003) reflection in Fig. 5 (b) corresponds to the number of domains with P_S oriented nearly parallel to the compression axis and the symmetry axis of the vertical integration segments. The intensity of (021) corresponds to the number of domains with P_S oriented ~71° and 109° away from the compression axis and fulfilling the diffraction conditions.

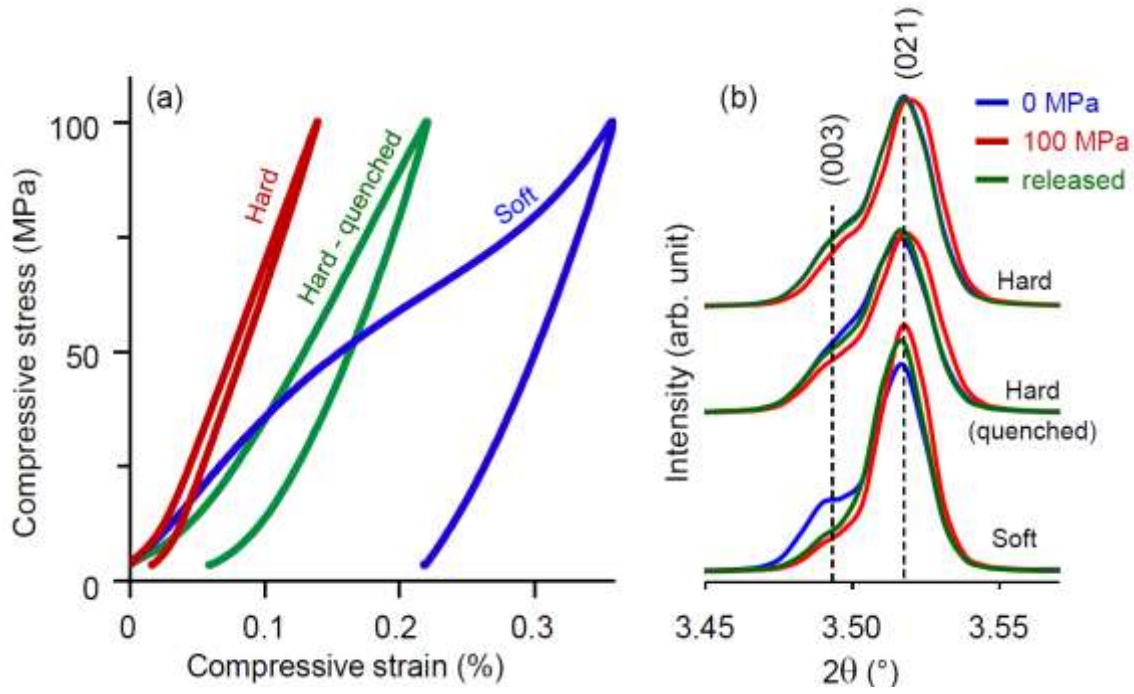

FIG. 5 Characterization of a single mechanical compression cycle for hard and soft compositions of rhombohedral $PbZr_{0.58}Ti_{0.42}O_3$ ceramics. (a) S-σ loops and (b) the corresponding (003) and (021) reflections in the "vertical" integration segment of X-ray diffraction.

The d-value of the split reflections due to non-cubic symmetry did not shift significantly during mechanical compression (Fig. 5 (b)), while single peaks such as d_{202} for the rhombohedral ceramics demonstrated a nonlinear and irreversible shift, as illustrated in Fig. 4 (c). This is likely an effect of compliance strain resulting from intergranular coupling,[46,47,54] and suggests that the soft rhombohedral ceramics are not fully relaxed after a compression cycle and, at least, some of the grains may remain stressed in the remanent state. This may partly be a reason why the experimentally examined macroscopic remanent strain may exceed the theoretical value calculated for an ideal polycrystalline material, as recently reported for some soft rhombohedral PZT compositions.[46,47]

Finally, in addition to the *in-situ* diffraction analysis performed in the transmission mode and allowing for investigation of domain switching processes in the bulk, we have also provided an *ex-situ* XRD analysis in the reflection mode prior and immediately after the mechanical testing. The *ex-situ* diffraction experiment aimed at investigation of domain switching at the surface normal to the compression axis. A typical example is shown in Fig. 6. Surprisingly, the behavior of ferroelastic domains at the surface appeared to be opposite to those in the bulk. The intensity ratio of the (003) and (021) reflections changed after compression where a pronounced increase in the intensity of the (003) reflection with higher d-spacing along the compression direction was clearly observed. Similar qualitative effects were systematically observed in all other investigated specimens representing hard, soft, rhombohedral, and tetragonal ceramics.

At present exact origin of this observation is unclear. The observed abnormal domain switching behavior at the surface may be a result of certain electrostatic conditions at the surface or clamping at the loading surface. Possible shear forces due to deviation from ideal parallel alignment of the ceramic sample and the compression fixture may contribute to the domain pattern at the surface, but the reproducibility of these observations point to that this is not an

artifact of the measurements. Further understanding of the observed phenomenon requires a more detailed investigation.

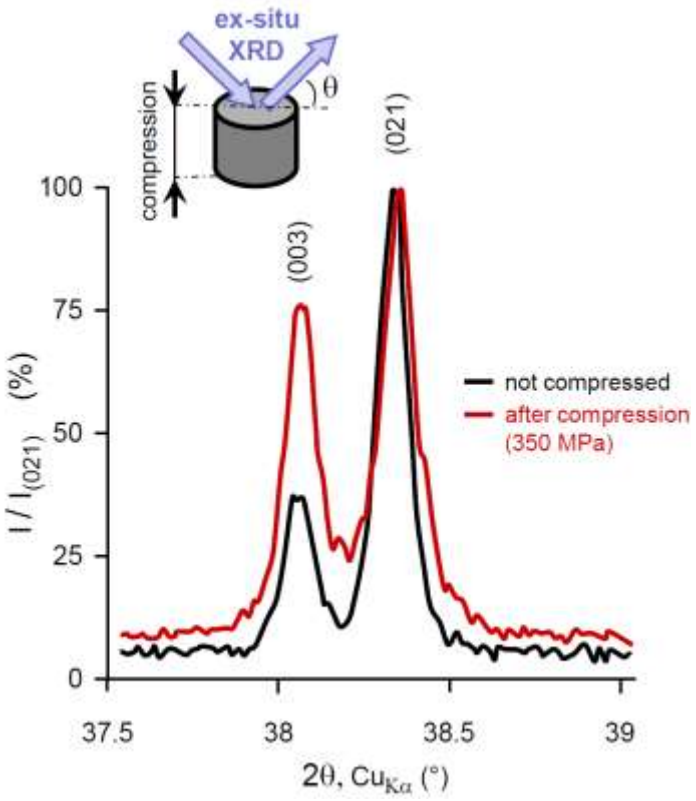

FIG. 6 Ex-situ X-ray diffraction patterns for soft rhombohedral PZT ceramics before and after mechanical compression. The patterns are diffraction from the outer surfaces normal to the compression axis (inset).

IV. SUMMARY

The ferroelectric and ferroelastic switching behavior in hard and soft PZT ceramics have been systematically investigated under cycling with electric field and mechanical compression. The acceptor and donor doping of soft and hard PZT was shown to affect the switching behavior of both the ferroelectric and the ferroelastic domains under mechanical or electrical fields

respectively. Switching of ferroelastic domains under mechanical compression was confirmed by *in-situ* X-ray diffraction. Thermal quenching of the originally hard ceramics was shown to soften both the mechanical and electrical properties. The observed behavior is rationalized in terms of extrinsic contribution of domain switching to ferroelectric and ferroelastic properties, consistent with the model of hardening-softening transition in ferroelectrics.

ACKNOWLEDGMENT

Financial support of the European Synchrotron Radiation Facility (ESRF) and the Norwegian Research Council, FRINATEK grant 197497 is acknowledged. PG and KGW gratefully acknowledge financial support from the Deutsche Forschungsgemeinschaft under WE 4972/1-1 and WE 4972/2-1. MM, MAE, and TG thank Thomas Buslaps for his valuable assistance at ESRF.

References

[1]B. Jaffe, W.R. Cook, and H. Jaffe, Piezoelectric Ceramics. 1971. New York: Academic.

[2]K. Carl and K. H. Hardtl, Ferroelectrics 17, 473 (1978).

[3]D.C. Lupascu, Yu. Genenko, and N. Balke, N., J. Am. Ceram. Soc. 89, 224 (2006).

[4] Yu.A. Genenko, J. Glaum, O. Hirsch, H. Kungl, M.J. Hoffmann, and T. Granzow, Phys. Rev. B 80, 224109 (2009)

[5]G.H. Jonker, J. Am. Ceram. Soc, 55, 57 (1972).

[6]A. Misarova, Solid State Phys., 2, 1160 (1960).

[7]V.S. Postnikov, V.S. Pavlov, and S.K. Turkov, Sov. Phys. - Solid State, 10, 1267 (1968)

[8]V.S. Postnikov, V.S. Pavlov, and S.K. Turkov, J. Phys. Chem. Solids, 31,1785 (1970).

[9]B.Q. Tan, J.-F. Li, and D. Viehland, Philos. Mag. B 76 59 (1997).

[10]Y. Zuo, Yu. A. Genenko, A. Klein, P. Stein, and B. Xu, J. Appl. Phys. 115, 084110 (2014).

[11]P. V. Lambeck and G. H. Jonker, Ferroelectrics 22, 729 (1978).

[12]U. Robels and G. Arlt, J. Appl. Phys., 73 3454 (1993)

[13]W.L. Warren, D. Dimos, G.E. Pike, K. Vanheusden, and R. Ramesh, Appl. Phys. Lett., 67, 1689 (1995).

[14]W.L. Warren, G.E. Pike, K. Vanheusden, D. Dimos, B.A. Tuttle, and J. Robertson, J. Appl. Phys., 79, 9250 (1996).

[15]W.L. Warren, K. Vanheusden, D. Dimos, G.E. Pike, and B.A. Tuttle, J. Am. Ceram. Soc., 79, 536 (1996).

[16]L.X. Zhang and X. Ren, Phys .Rev. B 71, 174108 (2005).

[17]M. Morozov, Ph.D. dissertation, Swiss Federal Institute of Technology – EPFL, 2006.

[18]P. Erhart, P. Träskelin, and K Albe, Phys .Rev. B 88, 024107 (2013).

[19]H. Mestric, R.-A. Eichel, K.-P. Dinse, A. Ozarowski, J. van Tol, and L. C. Brunel, J. Appl. Phys., 96, 7440 (2004).

[20]P. Erhart, R.-A. Eichel, P. Träskelin, and K. Albe, Phys. Rev. B 76, 174116 (2007).

[21]A. Chandrasekaran, D. Damjanovic, N. Setter, and N. Marzari, Phys. Rev. B 88, 214116 (2013).

[22]D. Damjanovic, "Hysteresis in piezoelectric and ferroelectric materials", in Science of Hysteresis (Eds G. Bertotti and I. Mayergoyz), Elsevier, pp. 337–465, 2005.

[23]S. Li, W. Cao, and L.E. Cross, J. Appl. Phys., 69 7219 (1991).

[24]Lord Rayleigh, R.S. XXV, Philos. Mag., 23, 225 (1887).

[25]L. Néel, Cahiers Phys., 12, 1 (1942).

[26]H. Kronmüller, Z. Angew. Phys., 30, 9 (1970)..

[27]O. Boser, J. Appl. Phys., 62, 1344 (1987).

[28]M. Morozov, D. Damjanovic, and N. Setter, J. Eur. Ceram. Soc. 25 2483 (2005).

[29]M.I. Morozov and D. Damjanovic, J. Appl. Phys. 104 034107 (2008)

[30]M.I. Morozov and D. Damjanovic, J. Appl. Phys. 107 034106 (2010)

[31]T.Rojac, M. Kosec, and D. Damjanovic, J. Am. Ceram. Soc. 94, 4108 (2011).

[32]T.Rojac, M. Kosec, B. Budic, N. Setter, and D. Damjanovic, J. Appl. Phys. 108, 074107 (2010).

[33]E. T. Wefring, F. H. Schader, K. G. Webber, M.-A. Einarsrud and T. Grande, submitted.

[34]D. Lin, K.W. Kwok, and H.L.W. Chan Appl. Phys. Lett. 90, 232903 (2007).

[35]C. Long, H. Fan, and M. Li, Appl. Phys. Lett. 103, 192908 (2013).

[36]D. Viehland and V.-H. Chen, Appl. Phys. 88, 6696 (2000).

[37]L. Jin, F. Li, and S. Zhang, J. Am. Ceram. Soc. 97, 1 (2014).

[38]D. Berlincourt, H. H. A. Krueger, and B. Jaffe, J. Phys. Chem. Solids, vol. 25, pp. 659-674, 1964.

[39]H. H. A. Krueger and D. Berlincourt, J. Acoust. Soc. Am., vol. 33, pp. 1339-1344, 1961.

[40]A.B. Schäufele and K.H. Härdtl, J. Am. Ceram. Soc. 79, 2637 (1996).

[41]M. Marsilius, K.G. Webber, E. Aulbach, and T. Granzow, J. Am. Ceram. Soc. 93, 2850 (2010).

[42]M. Marsilius, T. Granzow, and J.L. Jones, Sci. Technol. Adv. Mater. 12, 015002 (2011).

[43]F. H. Schader, M. Morozov, E. T. Wefring, T. Grande and K. G. Webber, J. Appl. Phys. 117, 194101 (2015).

[44]K.G. Webber, E. Aulbach, T. Key, M. Marsilius, T. Granzow, and J. Rödel, Acta Mater. 57, 4614 (2009).

[45]T. Leist, K.G. Webber, W. Jo, T. Granzow, E. Aulbach, J. Suffner, and J. Rödel, J. Appl. Phys. 109, 054109 (2011).

[46]Y.-H. Seo, D. Franzbach, J. Koruza, B. Malič, M. Kosec, J.L. Jones, and K.G. Webber, Phys. Rev. B 87, 094116 (2013).

[47]D. Franzbach, Y.-H. Seo, A.J. Studer, Y. Zhang, J. Glaum, J.E. Daniels, J. Koruza, A. Benčan, B. Malič, and K.G. Webber, Sci. Technol. Adv. Mater. 15, 015010 (2014).

[48]P.E. Vullum, J. Mastin, J. Wright. M.-A. Einarsrud, R. Holmestad, and T. Grande, Acta Mater. 54, 2615 (2006).

[49]A.P. Hammersley, ESRF Internal Report, ESRF97HA02T, Grenoble (1997).

[50]A.P. Hammersley, S.O. Svensson, M. Hanfland, A.N. Fitch, and D Häsermann, High Press Res. 14, 235 (1996).

[51]M. Davis, M. Budimir, D. Damjanovic, and N. Setter, J. Appl. Phys. 101, 054112 (2007).

[52]D. V. Taylor and D. Damjanovic, J. Appl. Phys. 82, 1973 (1997).

[53]D. Damjanovic and M. Demartin, J. Phys. D - Appl. Phys. 29, 2057 (1996).

[54]A. Pramanick, A.D. Prewitt, M.A Cottrell, W. Lee, A.J. Studer, K. An, C.R. Hubbard, and J.L. Jones, Appl. Phys. A 99 557 (2010).